

# Assembly of BaTiO<sub>3</sub> Nanocrystals into Macroscopic Aerogel Monoliths with High Surface Area\*\*

Felix Rechberger, Florian J. Heiligt, Martin J. Süess, and Markus Niederberger\*

**Abstract:** Aerogels with their low density and high surface area are fascinating materials. However, their advantageous morphology is still far from being fully exploited owing to their limited compositional variety and low crystallinity. Replacing the sol-gel process by a particle-based assembly route is a powerful alternative to expand the accessible functionalities of aerogels. A strategy is presented for the controlled destabilization of concentrated dispersions of BaTiO<sub>3</sub> nanoparticles, resulting in the assembly of the fully crystalline building blocks into cylindrically shaped monolithic gels, thereby combining the inherent properties of ternary oxides with the highly porous microstructure of aerogels. The obtained aerogels showed an unprecedentedly high surface area of over 300 m<sup>2</sup> g<sup>-1</sup>.

Aerogels are open-celled porous solid materials composed of a network of interconnected nanostructures with pores ranging up to 100 nm and a porosity of over 80%.<sup>[1]</sup> The production of conventional aerogels involves the direct gelation of a molecular precursor (typically metal alkoxides) in a sol-gel process. Extended hydrolysis and condensation beyond particle formation may eventually lead to a gel, an interconnecting porous network containing a continuous liquid phase. To keep the scaffold from collapsing during the removal of the liquid phase, a supercritical drying process is needed.<sup>[2,3]</sup> The obtained structures show an open porosity in a percolating network and as such feature a high surface area with a very low density. These characteristics led to the development of many types of aerogels for applications in catalysis, sensors, cosmic dust collectors, detectors in particle physics, thermal insulators, optoelectronic applications, and many more.<sup>[4,5]</sup> As a conductive matrix, aerogels could also be potentially applied in battery materials, capacitors, and as components in fuel- or solar cells.<sup>[5,6]</sup>

Despite this immense application potential, the advantageous morphological features of aerogels are far from being fully exploited, which is mainly due to the fact that their compositional variety is strongly limited to relatively simple metal oxides, and their low crystallinity is also a major issue. The reasons for these limitations can be found in the sol-gel process traditionally used for the preparation of aerogels. First, complex compositions are not only restricted by the lack of control over the hydrolysis and condensation rates of the molecular precursors, but also by the non-availability of suitable metal alkoxides. Second, gels obtained by the sol-gel route are amorphous and only heat treatment is able to induce crystallization. However, high-temperature annealing can lead to phase segregation, collapse of the porous structure, and breakdown of the monolithic body. One possibility to overcome these obstacles is to use preformed nanocrystals as building blocks. The major challenge in such an approach is the controlled gelling of the nanoparticles into a three-dimensional, percolating network that is mechanically stable enough to be further processed.

A promising strategy involves the controlled destabilization of the nanoparticles in dispersion, for example by partial removal of the surface stabilizing agent. Results supporting this strategy have been reported in 1997 by Boilot et al.<sup>[7]</sup> and a few years later by Brock et al.<sup>[8]</sup> for the preparation of semiconducting II-VI (CdS, CdSe, ZnS) and IV-VI (PbS) type aerogels. Despite significant efforts to expand the concept of preformed nanocrystalline building blocks to other materials, the composition of the aerogels remained limited to metal chalcogenides,<sup>[9]</sup> noble metals,<sup>[10]</sup> and their combinations.<sup>[11]</sup> Based on the observation that destabilization of surface functionalized titania nanoparticles induced oriented attachment preferentially in one direction and over several length scales,<sup>[12]</sup> we used this effect to prepare three-dimensionally connected titania aerogels from preformed anatase nanoparticles. Although we could extend this approach to multi-component aerogels, such as Au-TiO<sub>2</sub><sup>[13]</sup> and SiO<sub>2</sub>-TiO<sub>2</sub>,<sup>[14]</sup> they were always based on titania as matrix material owing to its strong tendency to undergo oriented attachment, which greatly facilitates the formation of porous gels. However, in terms of functional variety, it would be highly desirable to have other, possibly more complex oxides than titania, which could be gelled in a controlled way. Especially ternary oxides with their distinctive and diverse properties would be the ideal building blocks for the bottom-up synthesis of multifunctional aerogels for many technological applications.<sup>[15]</sup> Unfortunately, most of these oxides are not prone to oriented attachment and thus difficult to gel.

BaTiO<sub>3</sub> is one of the best known and most widely used oxide material for electroceramics owing to its excellent

[\*] F. Rechberger,<sup>[a]</sup> F. J. Heiligt,<sup>[a]</sup> M. J. Süess, Prof. Dr. M. Niederberger  
Laboratory for Multifunctional Materials  
Department of Materials, ETH Zürich  
Vladimir-Prelog-Weg 5, CH-8093 Zürich (Switzerland)  
E-mail: markus.niederberger@mat.ethz.ch

M. J. Süess  
Scientific Center for Optical and Electron Microscopy (SCOPM)  
Auguste-Piccard-Hof 1, CH-8093 Zürich (Switzerland)

[†] These authors contributed equally to this work.

[\*\*] The authors acknowledge the financial support by ETH Zurich (ETH 07 09-2). Furthermore, the support by the Scientific Center for Optical and Electron Microscopy (SCOPM) of ETH Zurich for TEM measurements as well as for providing a critical point dryer is greatly appreciated.

Supporting information for this article is available on the WWW under <http://dx.doi.org/10.1002/anie.201402164>.

piezo-, pyro-, and ferroelectric properties.<sup>[16]</sup> For other applications, such as in photocatalysis,<sup>[17]</sup> CO<sub>2</sub> reforming of CH<sub>4</sub>,<sup>[18]</sup> or in photoelectrochemistry,<sup>[19]</sup> a porous microstructure with large surface area would be preferred over a dense ceramic body. Up to now, the literature on possible applications of mesoporous BaTiO<sub>3</sub> is scarce, which is certainly also related to the difficulty to prepare such materials.

Mesoporous materials are typically prepared by sol-gel chemistry. However, BaTiO<sub>3</sub> is rather challenging to be synthesized by such a route, especially in crystalline form. The as-prepared amorphous gels have to be heated at least up to 600 °C to transform them into fully crystalline materials.<sup>[20,21]</sup> To remove traces of BaCO<sub>3</sub> impurities, typically present in sol-gel derived BaTiO<sub>3</sub>, even temperatures above 1000 °C are required.<sup>[22]</sup> Such an annealing step not only leads to considerable shrinkage of the gel, but can also change the Ba/Ti ratio.<sup>[20]</sup> Therefore, only very few BaTiO<sub>3</sub> aerogels have been reported so far. Demydov and Klabunde<sup>[23]</sup> showed the preparation of BaTiO<sub>3</sub> aerogels with 175 m<sup>2</sup> g<sup>-1</sup> surface area and a crystallinity of 82 % by hydrolysis and co-gelation of the corresponding metal alkoxides in an alcohol/toluene mixture. The assembly of preformed nanocrystalline BaTiO<sub>3</sub> particles into fully crystalline aerogels would therefore close a long-lasting gap in the synthesis of such highly porous structures. Because BaTiO<sub>3</sub> is a technologically important material, several viable synthesis routes to nanoscale particles with the appropriate particle size and narrow size distribution are available.<sup>[24–26]</sup> We made use of the nonaqueous sol-gel route, which has proven to give access to BaTiO<sub>3</sub> nanoparticles with high crystallinity.<sup>[27]</sup> Interestingly, these particles show a pronounced dipole moment in spite of their small size,<sup>[28–30]</sup> which makes them particularly attractive as nanoscale building blocks for assembly in an aerogel with unique functionality. Accordingly, the arrangement of nanoparticles into a macroscopic body opens up the fascinating option to combine the nano with the macro world.<sup>[5,31]</sup>

Here, we report the first liquid-phase and template-free assembly of crystalline BaTiO<sub>3</sub> nanoparticles into a highly porous, three-dimensionally connected network with macroscopic dimensions. The monolithic architecture with a cylindrical shape remained stable after supercritical drying and measured 1 × 1.5 cm exhibiting an unprecedentedly high surface area of over 300 m<sup>2</sup> g<sup>-1</sup>. The experimental details for the preparation of the BaTiO<sub>3</sub> nanoparticles and the assembly into an aerogel are given in the Supporting Information.

The synthesis of BaTiO<sub>3</sub> nanoparticles involved dissolving metallic barium in benzyl alcohol and adding the molar equivalent of titanium(IV) isopropoxide.<sup>[27]</sup> The mixture was then heated at 200 °C for 48 h, resulting in a white precipitate. Powder X-ray diffraction (PXRD) measurements (Figure 1 a) confirm the cubic phase of BaTiO<sub>3</sub> (ICDD PDF No. 01-070-9165). Laboratory X-ray diffraction is not sensitive enough to probe the local tetragonal distortion but it has been measured by synchrotron<sup>[30]</sup> and neutron diffraction<sup>[29]</sup> for the same samples. By using the Scherrer equation on the (110), (111), and (200) peaks, a crystallite size of 4 ± 1.9 nm was calculated. Figure 1b shows the microstructure of the BaTiO<sub>3</sub> nanoparticles observed by scanning electron microscopy (SEM) obtained by simply drying the as synthesized nanoparticles. It

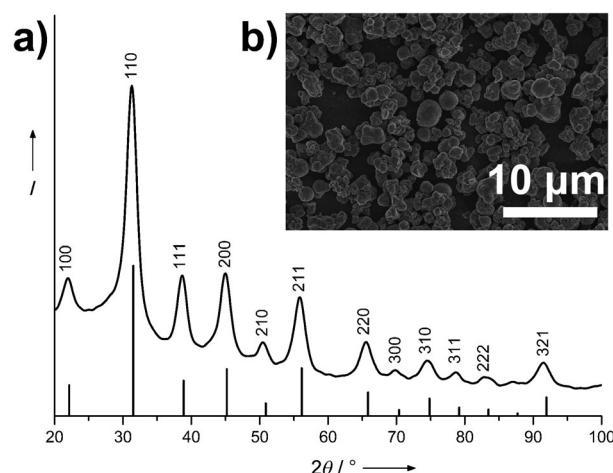


**Figure 1.** a) X-Ray diffractogram of the dried BaTiO<sub>3</sub> powder (solid bars: cubic BaTiO<sub>3</sub> reference, ICDD PDF No. 01-070-9165); b) scanning electron micrograph of the dried BaTiO<sub>3</sub> powder.

can be seen that the nanoparticles aggregate during drying and form spheres in the micrometer range.

The synthesized nanoparticles were functionalized with 2-[2-(2-methoxyethoxy)ethoxy]acetic acid (MEEAA) and dispersed in ethanol.<sup>[32]</sup> The gelling process itself is straightforward and does not involve any surface complexing agents or any chemical or photochemical oxidation of surface ligands.<sup>[5]</sup> The dispersion was simply destabilized by adding the same volumetric ratio of water, and the gelling process could then be induced either by heat or ultrasonic treatment. The characteristics of the aerogels are nearly identical for both methods, but the gelation time could be reduced by a factor of two when choosing ultrasonic treatment as gelation method. Figure 2 a shows a wet cylindrically shaped BaTiO<sub>3</sub> gel before supercritical drying and its dried counterpart retaining the macroscopic monolithic structure of 1 × 1.5 cm in size (Figure 2 b).

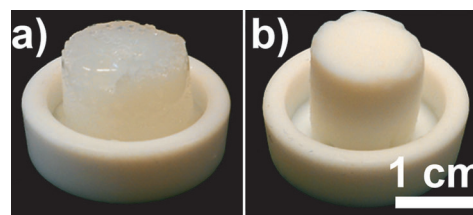


**Figure 2.** a) Photograph of a monolithic wet BaTiO<sub>3</sub> gel after gelling in a Teflon cup and b) the resulting aerogel after supercritical drying.

Because the electron microscopy results are representative for both preparation methods, only a sample treated by the ultrasonic method is shown. An overview SEM micrograph (Figure 3 a) of a supercritically dried aerogel reveals the homogenous and open-porous percolating network of BaTiO<sub>3</sub>. A close-up shows pillars of the aerogel scaffold measuring a few nanometers in size; thus the primary structures are, as intended, not densely packed (Figure 3 b). High-resolution transmission electron microscopy (HRTEM)

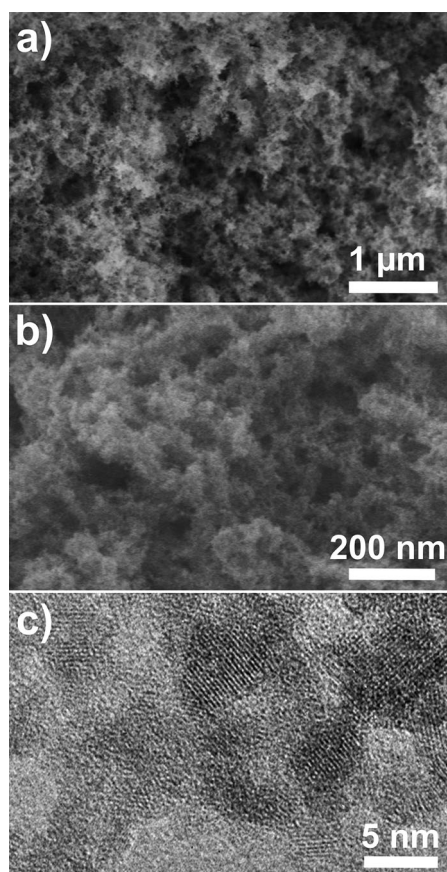


**Figure 3.** Micrographs of a BaTiO<sub>3</sub> aerogel obtained by electron microscopy techniques: a) SEM overview; b) SEM image at higher magnification; c) HRTEM image of a small section of the aerogel.

investigations confirmed the size of the single nanoparticles to be around 4 nm. The lattice fringes of the individual nanocrystals are randomly distributed with respect to each other, indicating that the network does not form by oriented attachment (Figure 3c). This observation is important, because it provides clear evidence that the gelation mechanism of BaTiO<sub>3</sub> is different to that observed for titania-based systems, although in both systems water plays a decisive role. In the case of titania, water promotes oriented attachment along [001] by selective destabilization of the corresponding crystal facets,<sup>[12]</sup> while here water leads to nonselective removal of MEEAA from the surface of the BaTiO<sub>3</sub> nanoparticles. Efficient destabilization was also the basis for the preparation of noble metal and metal chalcogenide aerogels from the corresponding nanoparticle dispersions,<sup>[5]</sup> but has hardly been reported yet for metal oxides. Although BaTiO<sub>3</sub> is just one example of such a rapidly induced destabilization process beyond oriented attachment, it indicates that this approach might be extendable to other metal oxide nanoparticles.

The nitrogen gas sorption measurements revealed properties of samples, which are not accessible by electron microscopy techniques. The gas sorption measurement results of MEEAA-functionalized BaTiO<sub>3</sub> based aerogels and the corresponding calculated values of porosity and density are summarized in Table 1 for all samples, where the gelling

**Table 1:** N<sub>2</sub> adsorption–desorption characteristics and calculations on BaTiO<sub>3</sub> aerogels with different gelling approaches.<sup>[a]</sup>

Gelling process	BET surface area [m <sup>2</sup> g <sup>−1</sup> ]	Pore volume [cm <sup>3</sup> g <sup>−1</sup> ]	Pore size [nm]	Density [g cm <sup>−3</sup> ]
HT	309.5 ± 8.6	2.02 ± 0.09	20.6 ± 1.3	0.34 ± 0.02
US	305.0 ± 3.3	2.17 ± 0.11	20.1 ± 0.4	0.32 ± 0.02

[a] HT: heat treatment, US: ultrasonic treatment.

process involved heat treatment (HT) or ultrasonication (US). The BET surface area obtained for BaTiO<sub>3</sub> powder (80.66 m<sup>2</sup> g<sup>−1</sup>) was significantly lower than the values of the BaTiO<sub>3</sub> aerogels (over 300 m<sup>2</sup> g<sup>−1</sup>), clearly proving different aggregation states. The large surface area and the clear hysteresis during desorption (see the Supporting Information, Figure S1) leads to the conclusion that pores must be present in the aerogels. The obtained surface areas are considerably higher than those found in literature on BaTiO<sub>3</sub> aerogels produced by co-gelation,<sup>[23]</sup> porous BaTiO<sub>3</sub> synthesized by polymer directed sol–gel templating,<sup>[33]</sup> and mesoporous BaTiO<sub>3</sub> by solvothermal methods.<sup>[34]</sup> Only calcined 2–3 nm-sized BaTiO<sub>3</sub> nanocrystals fabricated by a water based sol–gel process showed similarly high surface areas (286 m<sup>2</sup> g<sup>−1</sup>).<sup>[35]</sup> Pore sizes of 20 nm and pore volumes of around 2 cm<sup>3</sup> g<sup>−1</sup> were obtained by a density functional theory (DFT) analysis.<sup>[36]</sup> The achieved densities were calculated to be as low as 0.32 g cm<sup>−3</sup> for pores smaller than 227 nm, which is only 5 % of the bulk density of BaTiO<sub>3</sub> (6.08 g cm<sup>−3</sup>). The shape of the isotherm suggests the possibility of larger pores lying beyond the detection limit for gas sorption analysis and therefore leading to larger true pore volumes and consequently lower densities than calculated herein. In general, the pore sizes and the surface areas of the US-gelled samples are slightly smaller than the HT samples. However, the pore volume is slightly larger for the US aerogels. The pore size distribution of an US sample obtained by the DFT method is shown in the Supporting Information, Figure S2.

In summary, a powerful strategy is presented to self-assemble surface-functionalized BaTiO<sub>3</sub> nanocrystals into aerogel monoliths of macroscopic dimensions. The high crystallinity, fine nanostructure, porosity and large surface area makes this material interesting for applications beyond electroceramics.

The gelation mechanism is based on a rapidly induced destabilization of the BaTiO<sub>3</sub> nanoparticles in dispersion. The simplicity of the process and the fact that metal oxide nanoparticles prepared by the benzyl alcohol route<sup>[37]</sup> often have comparable surface characteristics suggest that it can be applied to other metal oxide nanoparticles, laying the foundation for a general synthesis strategy to crystalline oxide aerogels with broader compositional and functional variety.

Starting from nanoscale building blocks and ending with centimeter-sized bodies, the proposed bottom-up approach expands over seven orders of length scales, and the use of perovskite nanoparticles introduces another level of potential functionality. Although it is not yet possible to reliably investigate the properties of such functional aerogels, it can be expected that upon their availability also studies on their



properties and applications will be initiated, opening up a new field in aerogel research.

Received: February 7, 2014

Revised: April 24, 2014

Published online: May 22, 2014

**Keywords:** aerogels · barium titanate · mesoporous materials · self-assembly · sol-gel processes

- [1] J. Fricke, A. Emmerling in *Chemistry, Spectroscopy and Applications of Sol-Gel Glasses*, Vol. 77 (Eds.: R. Reisfeld, C. K. Jørgensen), Springer, Berlin, **1992**, pp. 37–87.
- [2] R. C. Mehrotra, A. Singh in *Progress in Inorganic Chemistry*, Wiley, Hoboken, **2007**, pp. 239–454.
- [3] N. Hüsing, U. Schubert, *Angew. Chem.* **1998**, *110*, 22–47; *Angew. Chem. Int. Ed.* **1998**, *37*, 22–45.
- [4] L. W. Hrubesh, *J. Non-Cryst. Solids* **1998**, *225*, 335–342.
- [5] N. Gaponik, A.-K. Herrmann, A. Eychmüller, *J. Phys. Chem. Lett.* **2011**, *3*, 8–17.
- [6] D. R. Rolison, B. Dunn, *J. Mater. Chem.* **2001**, *11*, 963–980.
- [7] T. Gacoin, L. Malier, J. P. Boilot, *Chem. Mater.* **1997**, *9*, 1502–1504.
- [8] J. L. Mohanan, I. U. Arachchige, S. L. Brock, *Science* **2005**, *307*, 397–400.
- [9] S. Bag, I. U. Arachchige, M. G. Kanatzidis, *J. Mater. Chem.* **2008**, *18*, 3628–3632.
- [10] N. C. Bigall, A.-K. Herrmann, M. Vogel, M. Rose, P. Simon, W. Carrillo-Cabrera, D. Dorfs, S. Kaskel, N. Gaponik, A. Eychmüller, *Angew. Chem.* **2009**, *121*, 9911–9915; *Angew. Chem. Int. Ed.* **2009**, *48*, 9731–9734.
- [11] T. Hendel, V. Lesnyak, L. Kühn, A.-K. Herrmann, N. C. Bigall, L. Borchardt, S. Kaskel, N. Gaponik, A. Eychmüller, *Adv. Funct. Mater.* **2013**, *23*, 1903–1911.
- [12] J. Polleux, N. Pinna, M. Antonietti, C. Hess, U. Wild, R. Schlögl, M. Niederberger, *Chem. Eur. J.* **2005**, *11*, 3541–3551.
- [13] F. J. Heiligt, M. D. Rossell, M. J. Stüss, M. Niederberger, *J. Mater. Chem.* **2011**, *21*, 16893–16899.
- [14] F. J. Heiligt, N. Kränzlin, M. J. Stüss, M. Niederberger, *J. Sol-Gel Sci. Technol.* **2014**, *70*, 300–306.
- [15] M. Niederberger, N. Pinna in *Metal Oxide Nanoparticles in Inorganic Solvents—Synthesis Formation, Assembly and Application*, Springer, London, **2009**, pp. 129–145.
- [16] J. Varghese, R. W. Whatmore, J. D. Holmes, *J. Mater. Chem. C* **2013**, *1*, 2618–2638.
- [17] L. Gomathi Devi, G. Krishnamurthy, *J. Phys. Chem. A* **2011**, *115*, 460–469.
- [18] T. Hayakawa, S. Suzuki, J. Nakamura, T. Uchijima, S. Hamakawa, K. Suzuki, T. Shishido, K. Takehira, *Appl. Catal. A* **1999**, *183*, 273–285.
- [19] S. Upadhyay, J. Shrivastava, A. Solanki, S. Choudhary, V. Sharma, P. Kumar, N. Singh, V. R. Satsangi, R. Shrivastav, U. V. Waghmare, S. Dass, *J. Phys. Chem. C* **2011**, *115*, 24373–24380.
- [20] H. Shimooka, M. Kuwabara, *J. Am. Ceram. Soc.* **1996**, *79*, 2983–2985.
- [21] R. Kaviani, A. Saidi, *J. Alloys Compd.* **2009**, *468*, 528–532.
- [22] M. Veith, S. Mathur, N. Lecerf, V. Huch, T. Decker, H. Beck, W. Eiser, R. Haberkorn, *J. Sol-Gel Sci. Technol.* **2000**, *17*, 145–158.
- [23] D. Demydov, K. J. Klabunde, *J. Non-Cryst. Solids* **2004**, *350*, 165–172.
- [24] L. Huang, Z. Chen, J. D. Wilson, S. Banerjee, R. D. Robinson, I. P. Herman, R. Laibowitz, S. O'Brien, *J. Appl. Phys.* **2006**, *100*, 034316.
- [25] C. W. Beier, M. A. Cuevas, R. L. Brutchey, *Small* **2008**, *4*, 2102–2106.
- [26] H. Du, S. Wohlrab, M. Weiss, S. Kaskel, *J. Mater. Chem.* **2007**, *17*, 4605–4610.
- [27] M. Niederberger, N. Pinna, J. Polleux, M. Antonietti, *Angew. Chem.* **2004**, *116*, 2320–2323; *Angew. Chem. Int. Ed.* **2004**, *43*, 2270–2273.
- [28] M. B. Smith, K. Page, T. Siegrist, P. L. Redmond, E. C. Walter, R. Seshadri, L. E. Brus, M. L. Steigerwald, *J. Am. Chem. Soc.* **2008**, *130*, 6955–6963.
- [29] K. Page, T. Proffen, M. Niederberger, R. Seshadri, *Chem. Mater.* **2010**, *22*, 4386–4391.
- [30] V. Petkov, M. Gateshki, M. Niederberger, Y. Ren, *Chem. Mater.* **2006**, *18*, 814–821.
- [31] D. Koziej, A. Lauria, M. Niederberger, *Adv. Mater.* **2014**, *26*, 235–257.
- [32] D. Taroata, W.-J. Fischer, T. A. Cheema, G. Garnweitner, G. Schmid, *IEEE Trans. Dielectr. Electr. Insul.* **2012**, *19*, 298–304.
- [33] W. Jiang, C. Jiang, X. Gong, Z. Zhang, *J. Sol-Gel Sci. Technol.* **2009**, *52*, 8–14.
- [34] B. Hou, Z. Li, Y. Xu, D. Wu, Y. Sun in *Stud. Surf. Sci. Catal., Vol. 156* (Eds.: S. Abdelhamid, J. Mietek), Elsevier, Dordrecht, **2005**, pp. 465–472.
- [35] M. R. Mohammadi, A. E. Rad, D. J. Fray, *J. Mater. Sci.* **2009**, *44*, 4959–4968.
- [36] J. Landers, G. Y. Gor, A. V. Neimark, *Colloids Surf. A* **2013**, *437*, 3–32.
- [37] N. Pinna, M. Niederberger, *Angew. Chem.* **2008**, *120*, 5372–5385; *Angew. Chem. Int. Ed.* **2008**, *47*, 5292–5304.